SEARCH FOR THE STANDARD MODEL HIGGS BOSON IN THE $HZ \to b\bar{b}\nu\bar{\nu}$ CHANNEL AT DØ

CHRISTOPHE OCHANDO
Laboratoire de l'Accélérateur Linéaire,
IN2P3-CNRS, Université Paris-Sud XI,
Bâtiment 200, 91898 Orsay Cedex, France.

A search for the standard model Higgs boson has been performed in 2.1 fb^{-1} of $p\bar{p}$ collisions at 1.96 TeV, collected with the DØ detector at the Fermilab Tevatron. The final state considered is a pair of b jets with large missing transverse energy, as expected from the reaction $p\bar{p} \to HZ \to b\bar{b}\nu\bar{\nu}$. The search is also sensitive to the $HW \to b\bar{b}\ell\nu$ channel, when the charged lepton is not identified. Boosted decision trees were used to discriminate the signal from the backgrounds, dominated by Wbb and Zbb final states. For a Higgs boson mass of 115 GeV, a limit has been set at 95% C.L. on the cross section times branching fraction of $(p\bar{p} \to H(Z/W)) \times (H \to b\bar{b})$, which is 7.5 times larger than the standard model value.

1 Introduction

The $p\bar{p} \to HZ$ reaction, with $H \to b\bar{b}$ and $Z \to \nu\bar{\nu}$, is among the most promising for the discovery of a low mass Higgs boson at the Fermilab Tevatron [1]. A search with 2.1fb^{-1} of data collected with the DØ detector is presentend here. A lower mass limit of 114.4 GeV was set by the LEP experiments for the Higgs boson from analyses of the reaction $e^+e^- \to HZ$ [2], while an upper limit of 144 GeV can be inferred from precision electroweak data [3]. Here and in the following, all limits quoted are at the 95% confidence level.

The final state topology considered in this analysis is a pair of b jets from the decay of the Higgs boson, with missing transverse energy ($\not\!\!E_T$) due to the neutrinos from the Z decay. The search is therefore also sensitive to the HW channel, with $W \to \ell\nu$ when the charged lepton from the W decay is not detected. The main backgrounds arise from $(W/Z)+$ jets, from top quark and diboson production and from multijet events produced by the strong interaction, with fake $\not\!\!E_T$ resulting from fluctuations in jet energy measurements and with real b or mistagged light parton jets.

A kinematic selection is first applied to reject most of the multijet events. The two jets expected from the Higgs boson decay are next required to be tagged as b jets, using a neural network b-tagging algorithm. Finally, discrimination between the signal and the remaining backgrounds is achieved by means of a boosted decision tree technique.

2 Data and Simulated samples

For this analysis, the data were recorded using a set of triggers designed to select events with jets and missing transverse energy. As the trigger conditions are not included into the full simulation, the calibration of the trigger response was performed on $Z \rightarrow \mu^+\mu^-$+jets events. Due to the muons which only deposit energy in the calorimeter at the minimum of ionization, these events have the same topology as the signal. Except for the background from multijet production, which was estimated from data, all backgrounds from the standard model (SM) were determined by Monte Carlo simulation.

3 Event Selection

3.1 Pre-Tagging Selection

At this stage, most of the cuts are applied to specifically reject the multijet background. The selected events are required to have:

- exactly 2 or 3 jets with $p_T > 20$ GeV and within $|\eta_{\rm det}| < 2.5$ [a]
- $\Delta\phi(\text{jet}_1, \text{jet}_2) < 165^\circ$ to avoid back-to-back jets in the plane transverse to the beam direction.
- $\not\!\!E_T > 50$ GeV. This criterion is tightened in case the direction of the missing E_T is close to the direction of one of the jets in the transverse plane: $\not\!\!E_T(\text{GeV}) > 80 - 40 \times \min\Delta\phi(\not\!\!E_T, \text{any jet})$, where the angle is measured in radians.
- The asymmetry $\mathcal{A} = (\not\!\!E_T - \not\!\!H_T)/(\not\!\!E_T + \not\!\!H_T)$, where $\not\!\!H_T = |-\Sigma\overrightarrow{p}_{T\text{jet}}|$, is required to lie between -0.1 and 0.2.
- In signal events, the missing track-p_T, $\not\!\!p_T$, defined as the opposite of the vectorial sum of the charged particle transverse momenta, is expected to point in a direction similar to that of the $\not\!\!E_T$. Advantage is taken of this feature by requiring $\Delta\phi(\not\!\!E_T, \not\!\!p_T) < \pi/2$.

To reject backgrounds from W+jets, top, and diboson production, events containing an isolated electron or muon are rejected.

3.2 Heavy-Flavor Tagging

Advantage is next taken of the large branching fraction for $H \rightarrow b\bar{b}$ by requiring the two leading jets to be b-tagged.

As can be seen in Fig. 1 for the invariant mass of the dijet system built from the two leading jets, the simulation provides a good description of the data both before (40 340 events expected and observed) and after (439 events observed and 442.8±1.1 expected) b-tagging. After b-tagging, the W+jets and Z+jets backgrounds are dominated by heavy flavor jet production, which contributes $\mathcal{O}(90\%)$.

4 Discriminant Analysis

In order to take full advantage of the different kinematic characteristics of the signal and background processes, a boosted decision tree (DT) technique [7] was used. A dedicated DT was trained for each of the Higgs boson masses probed and for each of the two data taking periods (these are Run IIa and Run IIb with different in experimental conditions).

The DT discriminants are shown in Fig. 2 for a Higgs boson mass of 115 GeV.

[a] $\eta_{\rm det}$ is the pseudorapidity measured from the detector center.

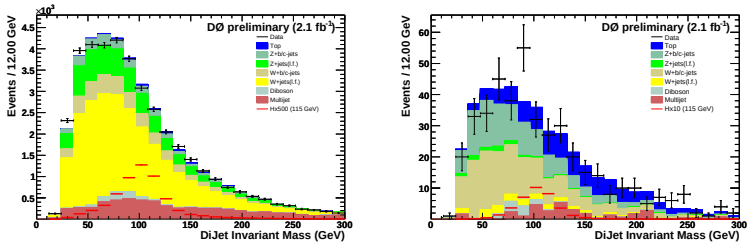

Figure 1: Distributions of the invariant mass of the two leading jets before (left) and after b-tagging (right). The data are shown as points with error bars. The various background contributions (SM and multijet) are shown as histograms, with color codes as indicated in the frames. Distributions for a signal with a Higgs boson mass of 115 GeV are also shown, multiplied by 500 before and by 10 after b-tagging.

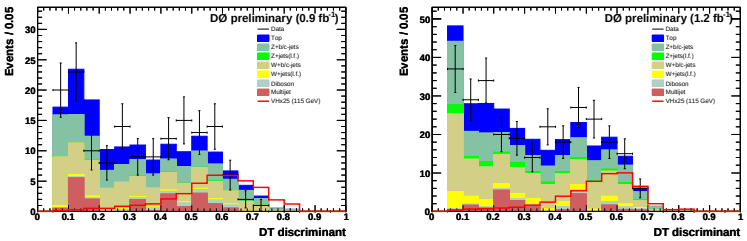

Figure 2: Distributions of the decision tree discriminants for a Higgs boson mass of 115 GeV (HZ and HW signals combined) for Run IIa (left) and Run IIb (right). The data are shown as points with error bars. The various background contributions (SM and multijet) are shown as histograms, with color codes as indicated in the frames. The distributions for the signal are multiplied by a factor of 25.

5 Systematic Uncertainties

Systematic uncertainties originate from various sources. Experimental uncertainties arise from the trigger simulation (5.5%), from the jet energy calibration (from 2% to 3%), resolution (about 1%), and reconstruction efficiency (2%), and from b-tagging (about 6%). Furthermore, a 6% error is assigned to the luminosity determination.

Moreover, the cross sections of the various SM and signal processes suffer from theoretical uncertainties. They were found to be at a level of 6 to 16%. They were estimated from MCFM [4] or from Refs. [5] and Ref. [6]. Finally, uncertainties on the heavy flavor fractions of W/Z+jets background(50%) are quoted.

6 Results

Agreement between data and expectation from SM and multijet backgrounds is observed both in terms of numbers of events selected and of DT discriminant shapes (Fig. 2). To set limits, based on the DT output, on the SM Higgs boson production cross section, a modified frequentist approach [8] was used.

The results obtained are shown as a function of the Higgs boson mass in Fig. 3 and in Table 1, in terms of the ratio of the excluded cross section times branching fraction for $H \to b\bar{b}$ to the SM Higgs prediction. The LLRs (Log Likelihood Ratios) are also shown in Fig. 3. For a 115 GeV Higgs boson mass, the observed and expected limits on the cross section of combined HZ and HW production times branching fraction for $H \to b\bar{b}$ are 7.5 and 8.4 times larger than the SM value, respectively.

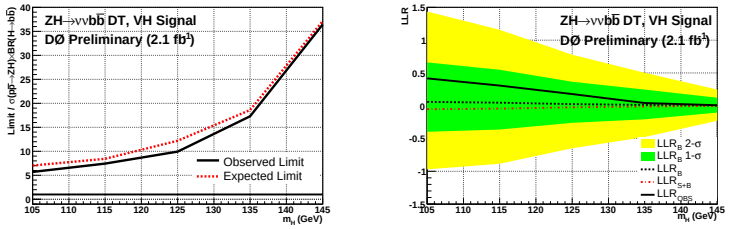

Figure 3: As a function of the Higgs boson mass, limit on the cross section of combined HZ and HW production times branching fraction for $H \to b\bar{b}$ (left), relative to the SM value, and log likelihood ratio (right). On the right, the observed and expected limits are shown as solid and dashed curves, respectively. On the left, the observed LLR is shown as a solid curve, the expected LLRs are shown as black and red dashed curves for the background-only and signal+background hypotheses, respectively, and the green and yellow areas correspond to the one and two σ deviations around the expected background-only LLR.

Mass (GeV)	105	115	125	135	145
Observed	5.7	7.5	9.9	17.3	36.4
Expected	7.0	8.4	12.2	18.6	37.1

Table 1: For various Higgs boson masses, observed and expected ratios of excluded to SM production cross sections times branching fraction for $H \to b\bar{b}$.

7 Summary

A search for the SM Higgs boson has been performed in 2.1 fb^{-1} of $p\bar{p}$ collisions at 1.96 TeV. The topology analysed consists of a pair of b jets with large $\not\!\!E_T$, as expected from $p\bar{p} \to HZ \to b\bar{b}\nu\bar{\nu}$. The search is also sensitive to HW production, where the W decays leptonically and the charged lepton is undetected. No deviation from the expectation from SM backgrounds was observed. A boosted decision tree technique was used to derive an upper limit on the cross section of the $p\bar{p} \to HZ$ and $p\bar{p} \to HW$ processes combined, as a function of the Higgs boson mass. For a mass of 115 GeV, this limit is a factor 7.5 larger than the SM cross section.

References

1. M. Carena *et al.*, *"Report of the Tevatron Higgs Working Group"*, arXiv:hep-ph/0010338; CDF and DØ Collaborations, *"Results of the Tevatron Higgs Sensitivity Study"*, FERMILAB-PUB-03/320-E.
2. R. Barate *et al.* [LEP Working Group for Higgs boson searches], Phys. Lett. B **565**, 61 (2003).
3. The LEP Collaborations: ALEPH Collaboration, DELPHI Collaboration, L3 Collaboration, OPAL Collaboration, the LEP Electroweak Working Group, *"Precision Electroweak Measurements and Constraints on the Standard Model,"* CERN-PH-EP/2007-039, arXiv:0712.0929v2.
4. J.M. Campbell and R.K. Ellis, Phys. Rev. D **60**, 113006 (1999).
5. M. Cacciari *et al.*, JHEP **404**, 068 (2004); N. Kidonakis and R. Vogt, Phys. Rev. D **68**, 114014 (2003); N. Kidonakis, Phys. Rev. D **74**, 114012 (2006).
6. S. Catani *et al.*, JHEP **0307**, 028 (2003).
7. L. Breiman *et al.*, *"Classification and Regression Trees"*, Wadsworth (1984); Y. Freund and R.E. Schapire, *"Experiments with a new boosting algorithm"*, in Machine Learning: Proceedings of the Thirteenth International Conference, pp. 148-156 (1996);
8. T. Junk, Nucl. Instrum. Methods in Phys. Res. A **434**, 435 (1999); A. Read, in *"1st Workshop on Confidence Limits,"* CERN Report No. CERN-2000-005, 2000.